Enchancing SOC Estimation Hybrid RNN Models for Li-Ion Batteries Under Various Temperatures

Ertuğrul Sert
Department of Computer Engineering
Ankara University[1]
Ankara, Türkiye
sertugrul18@hotmail.com

Bera Küçükkurt
Department of Computer Engineering
Ankara University[1]
Ankara, Türkiye
berakucukkurtjob@gmail.com

Atalay Bektaş
Department of Computer Engineering
Ankara University[1]
Ankara, Türkiye
atalaybektas@outlook.com

Umut Baran Ekinci
Department of Electrical Engineering
Istanbul Technical University[2],
Turkish Aerospace[3]
Ankara, Türkiye
ekinciu20@itu.edu.tr

Fatih Ekinci
Department of Computer Engineering,
Institute of Nuclear Sciences
Ankara University[1]
Ankara, Türkiye
fatih.ekinci@gsb.gov.tr

Koray Açıcı
Department of Artificial Intelligence and Data Engineering, Institute of Artifical Intelligence
Ankara University[1]
Ankara, Türkiye
kacici@ankara.edu.tr

2025 7th Global Power, Energy and Communication Conference (GPECOM) | 979-8-3315-1323-8/25/$31.00 ©2025 IEEE | DOI: 10.1109/GPECOM65896.2025.11061982

***Abstract*— Accurate estimation of State of Charge (SOC) across different temperatures is essential for ensuring the optimal performance and dependability of electrical systems, particularly in electric vehicles, Electrical Vertical Take-Off and Landing aircraft (eVTOLs), and smart devices. In this study, both hybrid and non-hybrid models are evaluated through a dynamically structured neural network to identify the most efficient approach for SOC prediction. The model architecture, which includes layer types, neuron counts, activation functions, and batch normalization, is optimized to enhance performance. A comparative analysis demonstrates that hybrid models achieve superior efficiency in SOC estimation, with lower Mean Absolute Error (MAE) values and enhanced generalization across varying temperature conditions. The findings indicate that combining various recurrent architectures enhances both adaptability and precision, making hybrid models a more effective and reliable option for SOC estimation. To further explore model performance, a dynamic model generation strategy was employed, enabling the construction of diverse architectures using real-world battery data collected under various driving cycles and temperature conditions. Among the evaluated models, the GRU-LSTM hybrid architectures achieved the lowest MAE values, demonstrating their improved generalization capability across diverse thermal and operational conditions.**

Keywords—Lithium-ion battery, State of Charge, Recurrent Neural Networks, Long Short-Term Memory, Gated Recurrent Unit, Neural Network

I. INTRODUCTION

In recent decades, electric vehicles (EVs), zero-emission aircraft and eVTOL aircrafts have gained significant attention in response to growing concerns about climate change, greenhouse gas emissions, and the exhaustion of fossil fuel resources, primarily due to their improved performance and efficiency [1]. On the one hand, the EV industry faces challenges due to energy storage system (ESS) limitations, on the other hand, lithium-ion batteries (LIBs) are favored for their high energy density, longevity, and efficiency with respect to the rise of the Li-ion technology. Therefore, a smart battery management system (BMS) is essential for optimal performance [2]. Monitoring the power system is a critical function of a BMS, with one of its key roles being the estimation of battery states. A primary state estimated is the SOC, which reflects the available capacity of the battery [3].

Deriving an accurate formula for SOC estimation is challenging. This is because the complexity of external factors, including voltage, current, battery or cell temperature, and their configurations, makes the process difficult [4]. Additionally, ambient temperature significantly influences the precision of SOC estimation, which is critical for accurately predicting the remaining driving range of EVs and optimizing charge-discharge management [5]. In LIBs applications, the voltage and current performance of the LIBs are affected by temperature and its variation [6]. Similarly, in hybrid unmanned aerial vehicles, rapid ambient temperature variations directly impact SOC estimation and energy management [7]. LIBs are essential for energy storage in electric aircraft, and accurately monitoring their SOC is key to ensuring the safety and efficient management of the aircraft's electrical systems [8].

Artificial neural networks (ANNs) are attracting growing attention for SOC estimation across diverse battery behaviors, fluctuating loads, and various temperatures [9,10]. Compared to traditional time series forecasting methods, deep learning approaches can better capture nonlinear relationships and long-term dependencies in complex data [1]. SOC estimation is fundamentally a time series prediction task, which is why recurrent neural networks (RNNs), known for their ability to process historical data, are commonly used in this area of research [11,12]. However, since RNNs struggle to capture long-term dependencies, the long short-term memory (LSTM) [13,14] and gated recurrent unit (GRU) [15,16] models, which incorporate gating mechanisms, were introduced to address this limitation.

The literature also explores various hybrid approaches for estimating SOC, such as the IBGRU-UKF method, which improves accuracy and robustness under various temperatures [17], the TFDAMN model, which leverages both time and frequency-domain features to enhance SOC estimation precision [18], the LSTM-GRU hybrid model, which facilitates accurate multi-step SOC predictions for real-world vehicle battery systems [19], and the LSTM-RNN model, incorporating extended input and limited output, which boosts the stability of SOC estimation through these methods [20].

979-8-3315-1323-8/25/$31.00 ©2025 IEEE

Authorized licensed use limited to: ULAKBIM UASL - ANKARA UNIVERSITESI. Downloaded on July 10,2025 at 12:17:42 UTC from IEEE Xplore. Restrictions apply.

Despite the promising advancements in deep learning based SOC estimation, several challenges persist. To overcome these challenges, this study employs a dynamic model generation approach, where the architecture is configured automatically through random selecting layer types (LSTM, GRU, RNN, Linear), along with decisions on the number of layers, neuron counts, activation functions, and batch normalization. This method enables the exploration of various model configurations, both hybrid and non-hybrid, to assess their performance. By generating these diverse architectures, the goal is to identify the most effective configurations for accurate and reliable SOC estimation under different environmental conditions, offering valuable insights into the trade-offs between hybrid and non-hybrid models.

The organization of the article is as follows: Section II describes the methods used, Section III introduces the dataset and experiments, Section IV discusses the results and comparisons of different solutions, and Section V concludes the study.

II. METHODS

A. State of Charge (SOC)

The expression of SOC has been present in academic literature since the 1960s [21]. Following its initial appearance, scholars have engaged in ongoing discussions regarding its definition. Despite these efforts, a universally accepted and precise definition has yet to be established [1].

$$SOC = \frac{Q_{current}}{Q_{max}} \times 100\% \quad (1)$$

Generally, SOC of a battery is described as the percentage of the battery's current available capacity $Q_{current}$ relative to its maximum capacity Q_{max} under specific conditions, such as temperature and charge/discharge rates. SOC formula is represented in Equation (1).

B. Recurrent Neural Network (RNN)

RNNs are a type of artificial neural network specifically developed to handle sequential data, such as time series information [22]. The structure of an RNN is represented in Fig. 1. Unlike a feedforward neural network, an RNN features a loop-like structure, achieved by incorporating recurrent units and establishing connections between hidden layers. This design enables memory retention, making it well-suited for handling time-sequence data.

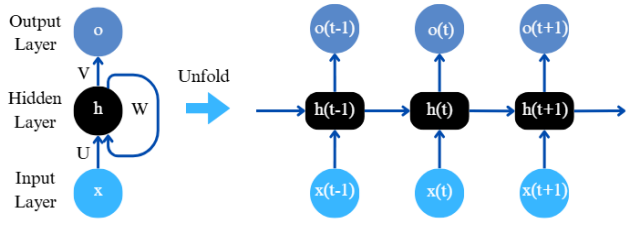

Fig. 1: Structure of the RNN

In Fig. 1, U, V, and W represent the weight matrices for input-to-hidden, hidden-to-output, and hidden-to-hidden connections, respectively. The input (x_t), hidden state (h_t), and output (o_t) at time (t). In equation (2) (σ) is an activation function (e.g. sigmoid or tanh) and b_h and b_o are the bias terms for the hidden and output layers, respectively.

$$h_t = (U_{x_t} + Wh_{t-1} + b_h)$$
$$O_t = \sigma(Vh_t + b_0) \quad (2)$$

However, RNNs struggle with challenges such as vanishing and exploding gradients when learning long-term dependencies. These challenges have led to the development of advanced variants such as LSTM [23] and GRU [24].

C. Long Short-Term Memory (LSTM)

LSTM networks are a specialized RNN designed to overcome the limitations of standard RNNs. In traditional RNNs [25], the effectiveness of LSTMs is due to their distinctive three-gate structure that governs the information flow within the network. These three gates are, the Forget Gate, which controls how much of the previous cell state is discarded; the Input Gate, which oversees the integration of new data into the cell state; and the Output Gate, which determines which part of the cell state will serve as the output for the next hidden state.

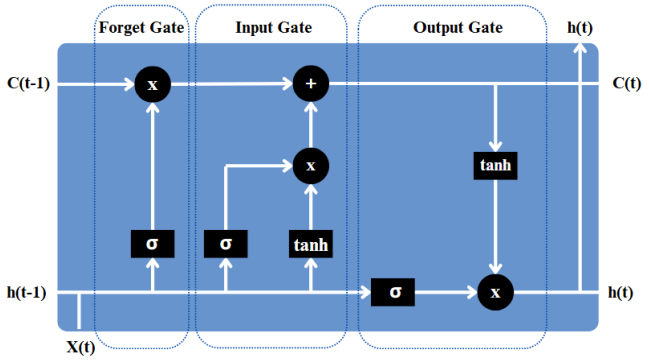

Fig. 2: Structure of the LSTM

The LSTM architecture is illustrated in Fig. 2. Mathematically, LSTM can be formulated as:

$$f_t = \sigma(W_f \cdot [h_{t-1}, x_t] + b_f)$$
$$i_t = \sigma(W_i \cdot [h_{t-1}, x_t] + b_i)$$
$$o_t = \sigma(W_o \cdot [h_{t-1}, x_t] + b_o)$$
$$\hat{C} = tanh(W_C \cdot [h_{t-1}, x_t] + b_C)$$
$$C_t = f_t * C_{t-1} + i_t * \tilde{C}_t$$
$$h_t = o_t * tanh(C_t) \quad (3)$$

The LSTM update process involves several operations to manage the flow of information. First, the forget gate (f_t) uses the previous hidden state (h_{t-1}) and the current input (x_t) to determine which portion of the cell state (C_{t-1}) to discard, employing a sigmoid activation. The input gate (i_t) and candidate cell state $(\tilde{C}_t)$ control the amount of new information added to the cell state. The cell state (C_t) is updated by integrating the previous state with new information, regulated by the forget gate. The output gate (o_t) then processes this updated cell state to produce the next hidden state (h_t), which acts as the output of the LSTM cell. These computations involve activation functions (σ) and tanh, with weight matrices and bias terms guiding the operations.

D. Gated Reccurent Unit (GRU)

GRU is a variant of RNN developed to overcome the vanishing gradient issue and effectively capture long-term dependencies [24]. While LSTM offers strong learning capabilities, its intricate structure leads to a higher computational cost. The GRU is a refined version of LSTM,

Authorized licensed use limited to: ULAKBIM UASL - ANKARA UNIVERSITESI. Downloaded on July 10,2025 at 12:17:42 UTC from IEEE Xplore. Restrictions apply.

delivering comparable performance. However, GRU features a simpler design, optimizing it for enhanced computational efficiency. and is faster to compute. The GRU consists of two gates: the update gate and the reset gate. The structure of a GRU is shown in Fig. 3, which is located below.

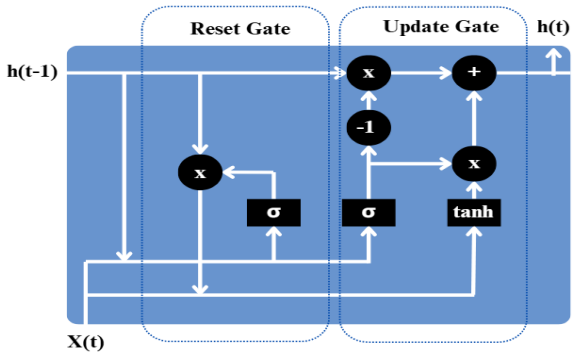

Fig. 3. Structure of the GRU

GRU formula expressed in Equation (4):

$$z_t = \sigma(W_z \cdot [h_{t-1}, x_t] + b_z)$$
$$r_t = \sigma(W_r \cdot [h_{t-1}, x_t] + b_r)$$
$$\hat{h}_t = tanh(W_h \cdot [r_t \cdot h_{t-1}, x_t] + b_h)$$
$$h_t = (1 - z_t) \cdot h_{t-1} + z_t \cdot \hat{h}_t \quad (4)$$

Using the activation function (σ), the update gate (z_t) decides how much of the previous hidden state (h_{t-1}) is carried forward. When determining the new candidate hidden state (h_t), the reset gate (r_t) and activation function regulate how much of the old state is eliminated. The tanh activation function is used to calculate the candidate state. Lastly, the update gate regulates how much of each state is used in the current hidden state (h_t), which is a combination of the candidate state and the preceding state.

E. Dynamic Model

This research adopts a dynamic model generation approach to explore various neural network architectures. Instead of manually defining a fixed structure, architectural types were randomly selected within predefined constraints, enabling a broader search space and evaluation of both hybrid and non-hybrid models to understand performance variations.

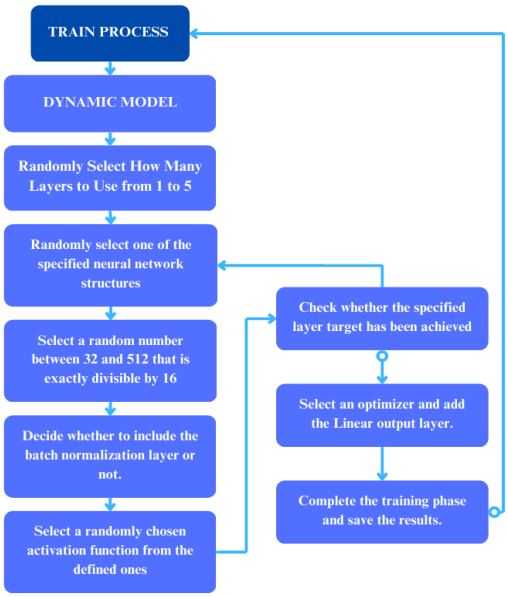

Fig. 4: Structure of the Dynamic Model

a) Layer Type and Number Selection: The selection of layer types is made from RNN, LSTM, GRU, and Linear layers, with the number of layers chosen between 1 and 5. For example, the model could first select an LSTM layer to process sequential data, followed by a GRU layer to further capture dependencies. Alternatively, the model might start with an RNN layer, and then use a Linear layer to adjust the output dimensions. This process allows for different combinations from a broad range of model architectures, including both non-hybrid and hybrid variants.

b) Number of Neurons Selection: The number of neurons in each layer is randomly selected as a multiple of 32, ranging from 32 to 512. This ensures a broad yet structured exploration of different configurations while maintaining randomness. For instance, an LSTM layer may be assigned 64 neurons, followed by a GRU layer with 128 neurons, enabling the model to evaluate diverse architectural variations.

c) Activation Selection: The activation function for each layer is randomly selected from options from ReLU, Tanh, Softplus, Softsign, or Sigmoid. For instance, the model may choose ReLU for a hidden, followed by Tanh. This randomized selection widens the space of possible model configurations, facilitates a more comprehensive exploration of network architectures.

d) Batch Normalization Selection: Finally, the decision to apply batch normalization or not is made randomly, further enhancing the exploration of diverse model architectures.

III. DATASET AND EXPERIMENT

A. Experimental Dataset

In this study, benchmark LIBs datasets from manufacturers, specifically the LG 18650 [28] is utilized. The publicly available dataset from the LG 18650 was tested across twelve different electric vehicle driving conditions at various temperatures. These conditions include four standard driving cycles—UDDS, HWFET, LA92, and US06 which are widely used to evaluate electric vehicle performance. Additionally, eight mixed driving conditions (Mixed 1–8) were generated by randomly combining these standard cycles. The key parameters of these batteries are summarized in the table below.

TABLE I BATTERY CELL SPECIFICATIONS

Type	**Battery Name**
	LG 18650
Anode	Graphite
Cathode	LNMC
Nominal Capacity	3 Ah
Current Cut-Off	50 mA
Voltage Cut-off	4.25V
Internal Impedance	≤20 mΩ
Weight	48g

The LG 18650 battery dataset consists of the following parameters: time (s), voltage (V), current (A), temperature (°C), capacity (Ah), time difference, and cumulative capacity (Ah). The LG 18650 battery dataset covers a temperature range from -20°C to 40°C.

Authorized licensed use limited to: ULAKBIM UASL - ANKARA UNIVERSITESI. Downloaded on July 10,2025 at 12:17:42 UTC from IEEE Xplore. Restrictions apply.

B. Training Procedure

The LG 18650 dataset does not provide direct SOC values. Instead, SOC was estimated by integrating two methodologies: the Open-Circuit Voltage (OCV) method, as described in Equation (5), and the Coulomb Counting (CC) method, as outlined in Equation (6).

$$SOC(t) = SOC(t_0) - \frac{1}{C_{actual}} \int_{t_0}^{t} I(t)dt \quad (5)$$

$$SOC(t) = SOC(t-1) + \frac{I(t)}{Q_n} \Delta t \quad (6)$$

A distinction was made between charging and discharging cycles to accurately model the battery's behavior under varying operational conditions. The OCV method was used to estimate the initial SOC values, followed by the Coulomb Counting technique, which continuously integrates the measured current over time, accounting for elapsed time and current flow to dynamically update SOC values.

Prior to training, Standard Scaling the Equation (7) was applied to normalize input features, ensuring a stable learning process.

$$X_{new} = \frac{X_i - X_{mean}}{X_{standart\ deviation}} \quad (7)$$

The model's input features included voltage, current, and temperature, with training conducted at four distinct temperatures: 0°C, 10°C, 25°C, and 40°C. The dataset was split into training and validation sets using data from Mixed 1-8 cycles. For testing, data from the UDDS and US06 cycles were utilized to evaluate model performance.

C. Evluation Metrics

The model's performance is evaluated using MAE Equation (8). MAE is also used as the loss function during validation.

$$MAE = \frac{1}{n} \sum_{i=1}^{n} |y_i - \hat{y}_i| \quad (8)$$

D. Dynamic Model Implentation

The model was implemented in Python and trained using the Adam optimizer with a learning rate of 0.001, a batch size of 512, and MAE loss as the objective function. Early stopping was applied with a patience of 5 epochs, and training was carried out for 50 epochs. The experiments were conducted in a Kaggle environment using an NVIDIA Tesla P100 GPU. The results from these experiments are outlined in the following section.

IV. Results and Discussions

This randomized approach enables the exploration of a diverse set of model architectures, encompassing various layer types, neuron configurations, activation functions, and batch normalization strategies. After training multiple models using these randomized configurations, the efficient architectures were selected. The details of these architectures and their corresponding results are presented in the following section. In the study, average MAE (%) is used as the evaluation metric to ensure a fair and comprehensive comparison by mitigating dataset-specific biases and providing a more generalized performance assessment across different conditions.

TABLE II MODELS COMPRASION LG DATASET MAE (%)

Models	Test Dataset	Temperatures				
		0 $C°$	**10 $C°$**	**25 $C°$**	**40 $C°$**	**AVG**
GRU-LSTM	UDDS	0.349	0.181	0.563	0.596	**0.301**
	US06	0.205	0.156	0.139	0.220	
RNN-GRU	UDDS	0.315	0.138	0.464	0.542	0.328
	US06	0.270	0.268	0.248	0.383	
LSTM-Linear	UDDS	0.351	0.134	0.430	0.535	0.330
	US06	0.236	0.237	0.290	0.433	
GRU-Linear	UDDS	0.363	0.201	0.436	0.615	0.339
	US06	0.314	0.256	0.280	0.251	
RNN- RNN	UDDS	0.205	0.208	0.411	0.477	0.340
	US06	0.300	0.339	0.470	0.307	
RNN	UDDS	0.153	0.159	0.496	0.433	0.343
	US06	0.197	0.199	0.591	0.516	
GRU	UDDS	0.484	0.168	0.394	0.441	0.349
	US06	0.261	0.234	0.333	0.475	
GRU-Linear-RNN	UDDS	0.679	0.167	0.202	0.266	0.356
	US06	0.302	0.248	0.451	0.539	
LSTM-GRU-GRU	UDDS	0.336	0.294	0.584	0.601	0.371
	US06	0.163	0.204	0.204	0.581	
LSTM	UDDS	0.206	0.195	0.744	1.007	0.383
	US06	0.222	0.244	0.184	0.264	

The results in Table II highlight the performance differences between hybrid and non-hybrid models in SOC estimation in variable temperature states. Hybrid models, which integrate multiple recurrent architectures such as LSTM, GRU, and RNN in a single structure, consistently demonstrate lower MAE values compared to standalone architectures. Specifically, the GRU-LSTM and RNN-GRU hybrid models achieve the lowest average MAE (%), indicating their ability to leverage complementary strengths from different network types. In contrast, non-hybrid models like LSTM and RNN exhibit higher error rates, suggesting limited adaptability to varying operational conditions. The enhanced generalization of hybrid models can be attributed to effectively capture both short-term and long-term dependencies within battery data. These findings reinforce the advantage of hybrid architectures in improving SOC estimation accuracy and reliability, making them a more reliable choice for practical applications.

Fig. 5 presents a comparison between the actual and predicted SOC values under different temperature conditions (0°C, 10°C, 25°C, and 40°C) for the UDDS driving cycle. The hybrid model demonstrates high estimation accuracy across all tested temperatures, with the predicted SOC closely following the actual trajectory. This indicates that the model can effectively capture SOC dynamics under normal operating conditions, such as 10°C and 25°C, maintaining reliable performance throughout the discharge cycle. The minimal deviation between the predicted and actual SOC values further emphasizes the model's accuracy and reliability in these typical conditions, with small variations observed at higher and lower temperatures, suggesting the model's adaptability to extreme environments.

Authorized licensed use limited to: ULAKBIM UASL - ANKARA UNIVERSITESI. Downloaded on July 10,2025 at 12:17:42 UTC from IEEE Xplore. Restrictions apply.

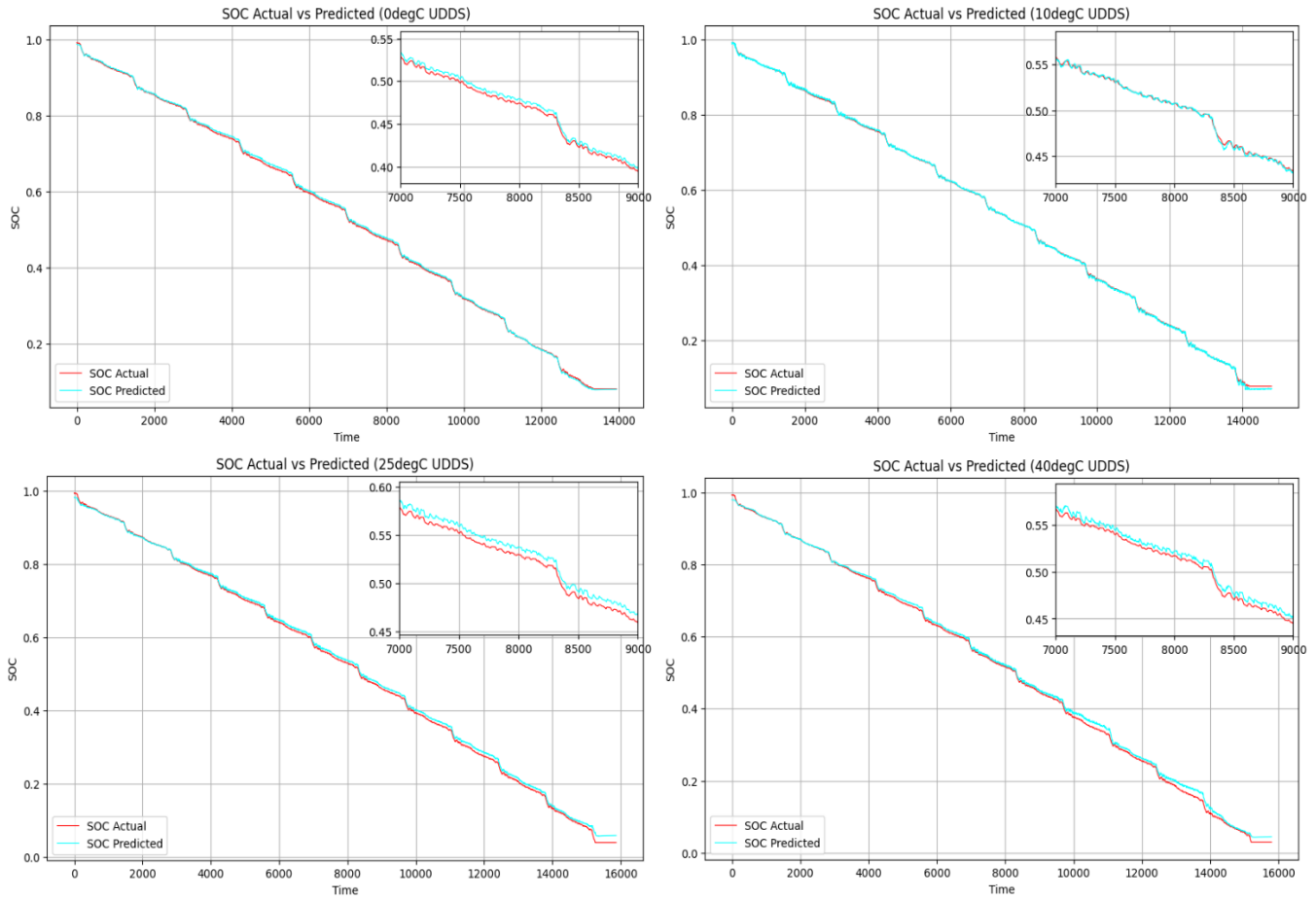

Fig. 5: SOC estimation using the hybrid GRU-LSTM model on UDDS test data

As Fig. 5 shows, slight discrepancies appear at extreme temperatures, where battery dynamics become more complex. Despite these minor variations, the predicted SOC values closely follow the actual trajectory, particularly at lower SOC levels. The minimal deviation between the curves suggests that the hybrid model effectively captures SOC dynamics and maintains stability across different temperatures. These results highlight the model's ability to generalize well, demonstrating its effectiveness for practical SOC estimation applications.

TABLE III LITERATURE COMPRASION LG DATASET MAE (%)

Models	Test Dataset	Temperatures				
		0 $C°$	**10 $C°$**	**25 $C°$**	**40 $C°$**	**AVG**
GRU-LSTM(Ours)	UDDS	0.349	0.181	0.563	0.596	0.422
	US06	0.205	0.156	0.139	0.220	0.180
Meta-Learning [26]	UDDS	-	-	-	-	1.45
	US06	-	-	-	-	1.01
IBGRU-UKF [17]	UDDS	0.76	0.54	0.50	0.67	0.617
	US06	0.76	0.54	0.50	0.67	0.617
TFDAMN [18]	UDDS	0.335	0.335	0.229	0.285	0.296
	US06	0.385	0.341	0.293	0.298	0.329
FNN [27]	UDDS	-	0.60	0.52	0.46	0.526
	US06	-	-	-	-	-

The results in Table III demonstrate that the proposed RNN-GRU model perform better than existing approaches. It shows a significantly lower MAE, surpassing Meta-Learning [26] and IBGRU-UKF [17], which display higher error rates across all conditions. Although TFDAMN [18] provides comparable results, the proposed model consistently delivers better accuracy, particularly for the US06 cycle. These findings indicate that the RNN-GRU hybrid model offers enhanced SOC estimation, making it a more effective solution across different temperatures and driving cycles.

V. CONCLUSION

This study introduces a dynamic model that combines both hybrid and non-hybrid architectures for SOC estimation in LIBs under various temperature conditions. The proposed approach utilizes a dynamic model generation strategy, which explores a wide range of possible architectures by randomly selecting different RNN-based layer types, neuron counts, activation functions, and batch normalization. This dynamic model allows for an extensive search space, enabling the adaptive construction of optimal architecture for accurate SOC prediction. The hybrid architectures, such as GRU-LSTM and RNN-GRU, are shown to performs better than non-hybrid models in terms of lower MAE and better generalization across various temperature conditions. The results suggest that combining multiple recurrent layers in hybrid models improves SOC estimation accuracy by capturing both short-term and long-term dependencies. This approach provides a reliable and scalable solution for BMS in EVs and eVTOLs, ensuring reliable SOC predictions under real-world operational conditions.

Future work will involve expanding the model to incorporate a broader range of temperature conditions and applying the different neural network structures to further enhance the SOC estimation accuracy.

Authorized licensed use limited to: ULAKBIM UASL - ANKARA UNIVERSITESI. Downloaded on July 10,2025 at 12:17:42 UTC from IEEE Xplore. Restrictions apply.

ACKNOWLEDGMENT

This study has been completed within the scope of the LIFT UP program of the Turkish Aerospace. Therefore, we sincerely appreciate their valuable assistance and support.

REFERENCES

[1] Hannan, M. A., Lipu, M. H., Hussain, A., & Mohamed, A. (2017). A review of lithium-ion battery state of charge estimation and management system in electric vehicle applications: Challenges and recommendations. *Renewable and Sustainable Energy Reviews*, *78*, 834-854.

[2] Ali, M. U., Zafar, A., Nengroo, S. H., Hussain, S., Junaid Alvi, M., & Kim, H. J. (2019). Towards a smarter battery management system for electric vehicle applications: A critical review of lithium-ion battery state of charge estimation. *Energies*, *12*(3), 446.

[3] Zhou, L., Lai, X., Li, B., Yao, Y., Yuan, M., Weng, J., & Zheng, Y. (2023). State estimation models of lithium-ion batteries for battery management system: status, challenges, and future trends. *Batteries*, *9*(2), 131.

[4] Hu, J. N., Hu, J. J., Lin, H. B., Li, X. P., Jiang, C. L., Qiu, X. H., & Li, W. S. (2014). State-of-charge estimation for battery management system using optimized support vector machine for regression. *Journal of Power Sources*, *269*, 682-693.

[5] Xing, Y., He, W., Pecht, M., & Tsui, K. L. (2014). State of charge estimation of lithium-ion batteries using the open-circuit voltage at various ambient temperatures. *Applied energy*, *113*, 106-115.

[6] Ekinci, U. B., & Kocabas, D. A. (2024, April). Investigation of the Effect of Pre-Heating on Performance Enhancement of Li-ion Batteries in Aviation Applications. In *2024 11th International Conference on Electrical and Electronics Engineering (ICEEE)* (pp. 265-269). IEEE.

[7] Luan, Z., Qin, Y., Hu, B., Zhao, W., & Wang, C. (2023). Estimation of state of charge for hybrid unmanned aerial vehicle Li-ion power battery for considering rapid temperature change. Journal of Energy Storage, 59, 106479.

[8] Bester, J. E., El Hajjaji, A., & Mabwe, A. M. (2015, November). Modelling of Lithium-ion battery and SOC estimation using simple and extended discrete Kalman Filters for Aircraft energy management. In IECON 2015-41st Annual Conference of the IEEE Industrial Electronics Society (pp. 002433-002438). IEEE.

[9] Xia, B., Cui, D., Sun, Z., Lao, Z., Zhang, R., Wang, W., ... & Wang, M. (2018). State of charge estimation of lithium-ion batteries using optimized Levenberg-Marquardt wavelet neural network. *Energy*, *153*, 694-705.

[10] Tang, X., Liu, K., Wang, X., Gao, F., Macro, J., & Widanage, W. D. (2020). Model migration neural network for predicting battery aging trajectories. *IEEE Transactions on Transportation Electrification*, *6*(2), 363-374.

[11] Feng, X., Chen, J., Zhang, Z., Miao, S., & Zhu, Q. (2021). State-of-charge estimation of lithium-ion battery based on clockwork recurrent neural network. *Energy*, *236*, 121360.

[12] Xi, Z., Wang, R., Fu, Y., & Mi, C. (2022). Accurate and reliable state of charge estimation of lithium ion batteries using time-delayed recurrent neural networks through the identification of overexcited neurons. *Applied Energy*, *305*, 117962.

[13] Ma, L., Hu, C., & Cheng, F. (2021). State of charge and state of energy estimation for lithium-ion batteries based on a long short-term memory neural network. *Journal of Energy Storage*, *37*, 102440.

[14] Almaita, E., Alshkoor, S., Abdelsalam, E., & Almomani, F. (2022). State of charge estimation for a group of lithium-ion batteries using long short-term memory neural network. *Journal of Energy Storage*, *52*, 104761.

[15] Jiao, M., Wang, D., & Qiu, J. (2020). A GRU-RNN based momentum optimized algorithm for SOC estimation. *Journal of Power Sources*, *459*, 228051.

[16] Wang, Y. X., Chen, Z., & Zhang, W. (2022). Lithium-ion battery state-of-charge estimation for small target sample sets using the improved GRU-based transfer learning. *Energy*, *244*, 123178.

[17] Cui, Z., Kang, L., Li, L., Wang, L., & Wang, K. (2022). A combined state-of-charge estimation method for lithium-ion battery using an improved BGRU network and UKF. *Energy*, *259*, 124933.

[18] Li, K., Zhang, Y., Liu, H., You, Y., Zeng, L., Hong, Y., ... & He, Z. (2024). A novel temporal-frequency dual attention mechanism network for state of charge estimation of lithium-ion battery. *Journal of Power Sources*, *622*, 235374.

[19] Hong, J., Liang, F., Yang, H., Zhang, C., Zhang, X., Zhang, H., ... & Yang, J. (2024). Multi-forword-step state of charge prediction for real-world electric vehicles battery systems using a novel LSTM-GRU hybrid neural network. *eTransportation*, *20*, 100322.

[20] Chen, J., Zhang, Y., Wu, J., Cheng, W., & Zhu, Q. (2023). SOC estimation for lithium-ion battery using the LSTM-RNN with extended input and constrained output. *Energy*, *262*, 125375.

[21] Li, Z., Huang, J., Liaw, B. Y., & Zhang, J. (2017). On state-of-charge determination for lithium-ion batteries. *Journal of Power Sources*, *348*, 281-301.

[22] Sherstinsky, A. (2020). Fundamentals of recurrent neural network (RNN) and long short-term memory (LSTM) network. *Physica D: Nonlinear Phenomena*, *404*, 132306.

[23] Hochreiter, S., and Schmidhuber, J.: 'Long short-term memory', Neural computation, 9, (8), 1997, pp. 1735-1780.

[24] Chung, J., Gulcehre, C., Cho, K., & Bengio, Y. (2014). Empirical evaluation of gated recurrent neural networks on sequence modeling. *arXiv preprint arXiv:1412.3555*.

[25] Bockrath, S., Rosskopf, A., Koffel, S., Waldhör, S., Srivastava, K., & Lorentz, V. R. (2019, October). State of charge estimation using recurrent neural networks with long short-term memory for lithium-ion batteries. In *IECON 2019-45th annual conference of the IEEE industrial electronics society* (Vol. 1, pp. 2507-2511). IEEE.

[26] Jeong, D., & Bae, S. (2023). Estimating battery state-of-charge with a few target training data by meta-learning. *Journal of Power Sources*, *553*, 232238.

[27] Khan, U., Kirmani, S., Rafat, Y., Rehman, M. U., & Alam, M. S. (2024). Improved deep learning based state of charge estimation of lithium ion battery for electrified transportation. *Journal of Energy Storage*, *91*, 111877.

[28] Kollmeyer, P., Vidal, C., Naguib, M., & Skells, M. (2020). LG 18650HG2 Li-ion battery data and example deep neural network xEV SOC estimator script. *Mendeley Data*, *3*(2020).

Authorized licensed use limited to: ULAKBIM UASL - ANKARA UNIVERSITESI. Downloaded on July 10,2025 at 12:17:42 UTC from IEEE Xplore. Restrictions apply.